BIOLOGICAL SCREENING FOR ANTI-INFLUENZA A VIRUS AGENTS

TAN MING CHEANG

FACULTY OF SCIENCE
UNIVERSITY OF MALAYA
KUALA LUMPUR

2018

BIOLOGICAL SCREENING FOR ANTI-INFLUENZA A VIRUS AGENTS

TAN MING CHEANG

DISSERTATION SUBMITTED
IN FULFILMENT OF THE REQUIREMENTS FOR THE
DEGREE OF MASTER OF SCIENCE

INSTITUTE OF BIOLOGICAL SCIENCES
FACULTY OF SCIENCE
UNIVERSITY OF MALAYA
KUALA LUMPUR

2018

UNIVERSITY OF MALAYA

ORIGINAL LITERARY WORK DECLARATION

Name of Candidate: Tan Ming Cheang

Matric No: SGR 130049

Name of Degree: Master of Science

Title of Thesis: Biological Screening for Anti-Influenza A Virus Agents

Field of Study:

I do solemnly and sincerely declare that:

(1) I am the sole author/writer of this Work;
(2) This Work is original;
(3) Any use of any work in which copyright exists was done by way of fair dealing and for permitted purposes and any excerpt or extract from, or reference to or reproduction of any copyright work has been disclosed expressly and sufficiently and the title of the Work and its authorship have been acknowledged in this Work;
(4) I do not have any actual knowledge nor do I ought reasonably to know that the making of this work constitutes an infringement of any copyright work;
(5) I hereby assign all and every rights in the copyright to this Work to the University of Malaya ("UM"), who henceforth shall be owner of the copyright in this Work and that any reproduction or use in any form or by any means whatsoever is prohibited without the written consent of UM having been first had and obtained;
(6) I am fully aware that if in the course of making this Work I have infringed any copyright whether intentionally or otherwise, I may be subject to legal action or any other action as may be determined by UM.

Candidate's Signature Date:

Subscribed and solemnly declared before,

Witness's Signature Date:

Name:

Designation:

BIOLOGICAL SCREENING FOR ANTI-INFLUENZA A VIRUS AGENTS

ABSTRACT

Influenza virus is estimated to cause 3-5 million severe complications and about 250-500 thousand deaths per year. Different kinds of anti-influenza virus drugs have been developed. However, the emergence of drug resistant strains has presented a big challenge for efficient antiviral therapy. Indole derivatives have been shown to exhibit both antiviral and anti-inflammatory activities. In this study, a cell-based system was adopted to screen for potential anti-IAV agents. Four indole derivatives (named 525A, 526A, 527A and 528A) were subjected to the antiviral screening, of which 526A was selected for further investigation. Here, pre-treating cells with 526A protects adenocarcinomic human alveolar basal epithelial cells from IAV infection. Furthermore, 526A inhibits IAV replication by inhibiting the expression of IAV genes. Interestingly, 526A partially blocks the activation of RIG-I pathway and therefore suppresses the activation of IRF3 and STAT1 in host cells and thus represses the production of type I interferon response and cytokines in IAV-infected cells. Taken together, these results suggest that 526A may be a potential anti-influenza A virus agent.

Keywords: IAV, indole, 526A

PENYARINGAN BIOLOGI BAGI AGEN ANTI-VIRUS INFLUENZA A

ABSTRAK

Virus influenza dianggar mengakibatkan 3-5 juta komplikasi yang teruk dan kira-kira 250-500 ribu kematian setiap tahun. Pelbagai jenis vaksin virus anti-influenza telah ditemui dan dihasilkan. Namun begitu, keberkesanan terapi vaksin anti-influenza kerap dicabar dengan kemunculannya rintangan strain. Terdapat sesetengah terbitan indole mempunyaikan aktiviti anti-virus dan anti-radang. Dalam kajian ini, sistem saringan yang berasaskan sel digunakan untuk mengetahui agen anti-IAV yang berpotensi. Empat terbitan indole (yang dinamakan 525A, 526A, 527A dan 528A) telah digunakan untuk mengkaji activiti anti-virus dan di antaranya, 526A telah dipilih untuk kajian lanjut. Didapati bahawa pra-rawatan sel-sel dengan 526A akan melindungi sel-sel epitelium adenokarsinoma alveolar basal manusia daripada jangkitan IAV. Tambahan pula, replikasi IAV telah direncatkan oleh 526A melalui pengurangan ekspresi gen IAV dan protein. Perkara yang menarik adalah bahawa sebahagian pengaktifan laluan RIG-I juga didapati terhalang oleh 526A dan menjejaskan pengaktifan IRF3 dan STAT1 dalam sel normal dan menyekat pengeluaran interferon jenis I dalam sel-sel yang telah dijangkiti oleh IAV. Kesimpulannya, data ini menunjukkan bahawa 526A merupakan satu ejen anti-influenza A virus yang berpotensi.

Kata Kunci: IAV, indole, 526A

ACKNOWLEDGEMENTS

Many people have contributed to my work here at University of Malaya. I am grateful to have the research funding from the University of Malaya High Impact Research Grant (UM.C/625/1/HIR/MOHE/CHAN-02) and the University Malaya Postgraduate Research Grant (PG136-2014B) which made this project possible.

To my deepest sense of gratitude I am very thankful to Chee-Kwee Ea for supervising me several years before pursuing his further career at USA. He has shared with me many tips on multitasking and the proper way of data troubleshooting, which layer a good research foundation in me. Also, thank you my supervisor Yat-Yuen Lim for the guidance as well as providing many helpful suggestions to complete my project.

I thank Hapipah Mohd Ali and her team for sharing with me the chemical compounds. I am thankful to Jesse Bloom (Fred Hutchinson Cancer Research Center, USA) who provides the studying materials (eg. the PR8-PB1flank-eGFP virus, the A549-PB1 cells and the 293T-PB1 cells). I want to thank Glen N. Barber (University of Miami, USA) for the VSV-GFP source too.

Next, I would like thank Taznim Begam Mohd Mohidin for the support in various capacities. To my helpful and friendly Epigenetics lab mates (Kok Siong, Wei Lun, Wan Ying and Sheng Wei), appreciate for your experience and knowledge sharing throughout my time in the Epilab. And thank you Gabriel Pineda (National University, USA) for the comments and the critical reading of my manuscript.

Besides, I would like to thank the University of Malaya High Impact Research Department for the good research facilities and excellent research environment.

Lastly, I would like to thank my family for moral support.

TABLE OF CONTENTS

LIST OF FIGURES

LIST OF TABLES

LIST OF SYMBOLS AND ABBREVIATIONS

α	- Alpha
A	- Ampere
β	- Beta
˚C	- Degree Celsius
κ	- Kappa
l	- Litre
µ	- Micro
m	- Milli
M	- Molar
%	- Percentage
A549	- Adenocarcinomic human alveolar basal epithelial cells
ATP	- Adenosine triphosphate
BSA	- Bovine serum albumin
CARDs	- Caspase activation and recruitment domains
CO_2	- Carbon dioxide
CRM1	- Chromosomal maintenance 1
DMSO	- Dimethyl sulfoxide
eGFP	- Enhanced green fluorescent protein
FACS	- Fluorescence-activated cell sorting
FSC	- Forward scatter
HEK	- Human embryonic kidney cells
HRP	- Horseradish peroxidase
IAV	- Influenza A virus

IB - Immunoblotting

IC50 - Inhibitory concentration of half maximal

IFIT2 - Interferon induced protein with tetratricopeptide repeats 2

IFN - Interferon

IL6 - Interleukin 6

IP - Infectious particle

IP10 - Interferon gamma-induced protein 10

IRF - Interferon regulatory factor

LRR - Leucine-rich repeat

M1 - Matrix protein 1

M2 - Matrix protein 2

MAVS - Mitochondrial antiviral signalling protein

MDA5 - Melanoma Differentiation-Associated protein 5

MOI - Multiplicity of infection

MTT - 3-(4, 5-dimethylthiazol-2-yl)-2, 5-diphenyltetrazolium bromide

NA - Neuraminidase

NBD - Nucleotide-binding domain

NEP - Nuclear export protein

NF-κB - Nuclear factor kappa B

NOD - Nucleotide-binding oligomerization domain

NP - Nucleoprotein

NSP1 - Non-structural protein 1

NSP2 - Non-structural protein 2

PA - Polymerase acidic protein

PAMPs - Pathogen-associated molecular patterns

PB1 - Polymerase basic protein 1

PB2 - Polymerase basic protein 2

PBS - Phosphate saline buffer

PKR - Protein kinase RNA-activated

PRRs - Pattern recognition receptors

RdRp - RNA dependent RNA Polymerase

RIG-I - Retinoic acid-inducible gene- I

RNA - Ribonucleic acid

SDHA - Succinate dehydrogenase complex, subunit A

STAT1 - Signal transducer and activator of transcription 1

TLRs - Toll like receptors

TNF - Tumor necrosis factor

TPCK - Tosyl phenylalanyl chloromethyl ketone

vRNP - Viral ribonucleoprotein

VSV - Vesicular stomatitis virus

LIST OF APPENDICES

CHAPTER 1: INTRODUCTION

Influenza (flu) is a disease that is caused by contagious viral infection which mainly infects respiratory tract of many animals, birds and humans. In tropical regions, outbreak of influenza diseases may occur throughout the year and may cause financial burden due to health care cost and productivity lost. The world experienced four influenza pandemics which were Spanish flu in 1919, Asian flu in 1957, Hong Kong flu in 1968 and H1N1 in 2009. Annually, 5 - 10 % of adults and 20 - 30 % of children are vulnerable to influenza infection according to the World Health Organization. Worldwide, influenza is estimated to cause 3 to 5 million severe complications and about 250 000 to 500 000 deaths every year.

There are three types of influenza viruses – A, B and C, which are categorized based on the variation in the nucleoprotein antigen. Recent appearance of Influenza A Virus strains such as H1N1 and H5N1 avian influenza alert the community to study in more details about the IAV infections and the immune response to control and prevent IAV infection. Antiviral drugs play a vital role in fast-spreading epidemics such as influenza A virus (IAV). However, owing to the continuous evolution of major viral antigens that lead to drug resistance and low efficacy to treatment, the focus on discovering an effective anti-influenza drug is extremely crucial to counter act on the existing influenza pandemics as well as new pandemic strains.

Indole is an aromatic heterocyclic organic compound with a bicyclic structure consisting of a six-membered ring fused to a five-membered nitrogen-containing pyrrole ring. In this study, four novel synthetic indole derivative agents are used to screen for their anti-influenza A virus activities on adenocarcinomic human alveolar basal epithelial cells that stably express PB1 gene (A549-PB1). This thesis provides an understanding on the interactions of the indole derivatives towards several viral proteins

in the cells. This investigation on the biological activity of 526A on A549-PB1 cells can be very beneficial and important for discovering new antiviral agents.

The objective of this study is to screen four indole derivative compounds for anti-influenza A virus activity. Specifically, the objectives are as below:

1) To determine the cytotoxicity (IC_{50}) of these compounds on A549-PB1 cells.
2) To screen the compound that possesses anti-influenza A virus property using a cell-based screening assay.
3) To understand the biological activity of IAV-infected A549-PB1 cells after compound treatment.

CHAPTER 2: LITERATURE REVIEW

2.1 Influenza Virus

Influenza is a member of the *Orthomyxoviridae* family. There are three types of influenza viruses – A, B and C. Among all, type A influenza virus draws the most attention as it is the most virulent and highly infectious compared to influenza B and C viruses. Influenza A is a negative sense, single-stranded and segmented ribonucleic acid (RNA) virus (Samji, 2009). It has eight segments (Figure 2.1) that encode for a few viral genes, such as hemagglutinin (HA), neuraminidase (NA), matrix protein 1 (M1), matrix protein 2 (M2), nucleoprotein (NP), non-structural protein 1 (NSP1), non-structural protein 2 (NSP2; also known as nuclear export protein, NEP), polymerase acidic protein (PA), polymerase basic protein 1 (PB1), and polymerase basic protein 2 (PB2) (Gao et al., 2012). Based on HA and NA, IAVs can be categorized into 18 antigenic HA (H1-H18) subtypes and 11 NA (N1-N11) subtypes.

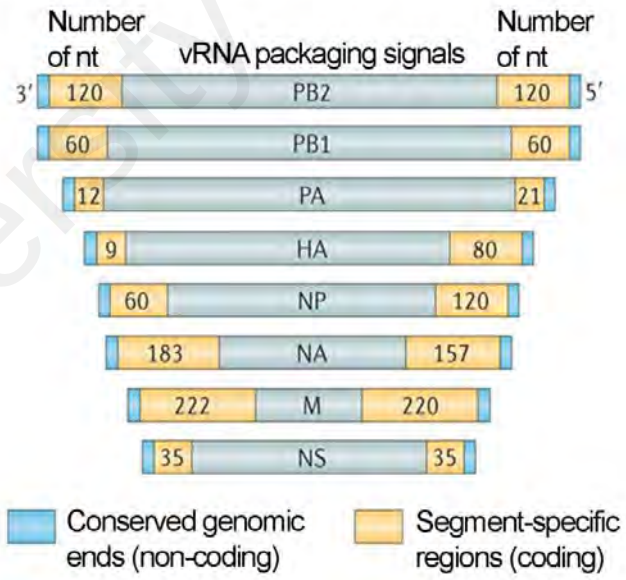

Figure 2.1: Eight influenza A virus (IAV) vRNP segments.
Structure of eight segmented IAV genome (nt: nucleotide) (Eisfeld et al., 2015).

2.2 Structure of IAV

IAV is an enveloped virus as its outer layer is a lipid bilayer membrane that is taken from a host cell in aiding the viral survival and infection to other cells. This lipid bilayer carries three viral transmembrane proteins: HA, NA and M2. Underneath the membrane is a layer of M1 and the core viral ribonucleoprotein (vRNP) complexes, which consist of viral RNAs, heterotrimeric polymerase complex and nucleoprotein (Figure 2.2).

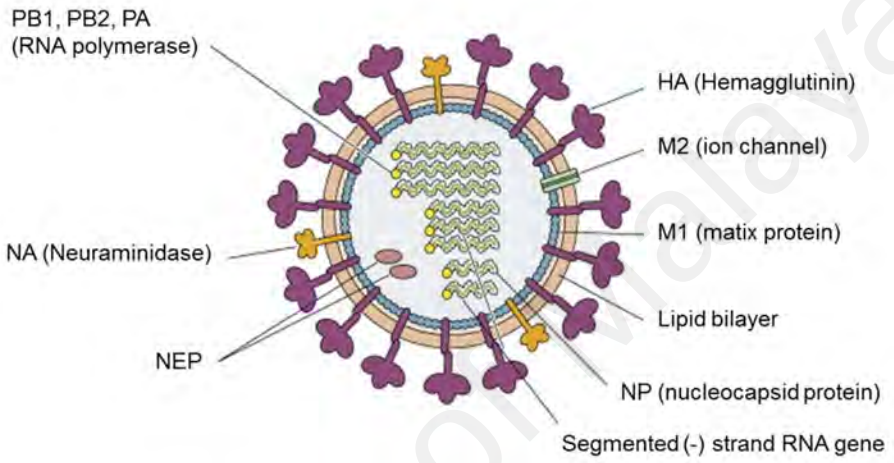

Figure 2.2: Structure of Influenza A virus.
(Source: http://www.virology.ws/2009/04/30/structure-of-influenza-virus/)

2.3 IAV Life Cycle

HA molecule, which forms a trimer, is distributed on viral lipid membrane in the form of a spike-like structure. The HA precursor, HA0, consists of two subunits: HA1, which has a sialic acid binding site, and HA2, which possesses a fusion motif. When IAV encounters a normal host cell, binding of viral surface glycoprotein HA1 to the host cell-surface sialic acid receptors induces endocytosis of the virus. The influx of protons via M2 ion channel decreases the pH in the vesicle that further leads to a structural change in the HA0, and activates the exposed HA2 for the membrane fusion process (Samji, 2009). Thereby, the vRNPs will be released from M1 of the viral core into the cytoplasm of cells and then further transported into the cell nucleus (Figure 2.3).

As a negative sense strands of RNA, the viral genome will be converted into a positive sense RNA in the cell nucleus, serving as a template for viral RNAs production. Replication of viral genome requires the viral RNA-dependent RNA polymerase (RdRp), which is a heterotrimer which consists of PA, PB1 and PB2. The PA subunit possesses endonuclease and protease activities while the PB1 subunit catalyzes the activity of nucleotide elongation and it also interacts with both PA and PB2 (Das et al., 2010; Nakagawa et al., 1996). The PB2 subunit has endonuclease activity and the ability to recognize the cap structure of host cell RNA (Nakagawa et al., 1996). The viral RNA polymerase utilizes "cap-snatching" mechanism to synthesize viral mRNA with 5' methylated capped RNA fragment cleaved from host pre-mRNA (Das et al., 2010).

The viral mRNAs will be transported to the cytoplasm to produce viral proteins, such as HA, M2 and NA (Samji, 2009). Negative sense vRNPs are exported from the nucleus via CRM1 dependent pathway (Samji, 2009). As an enveloped virus, IAV uses host cell's plasma membrane to form viral particles and leaves the infected cell (Das et al., 2010). The newly synthesized NA helps to release the new virus by cleaving the sialic acids (Samji, 2009).

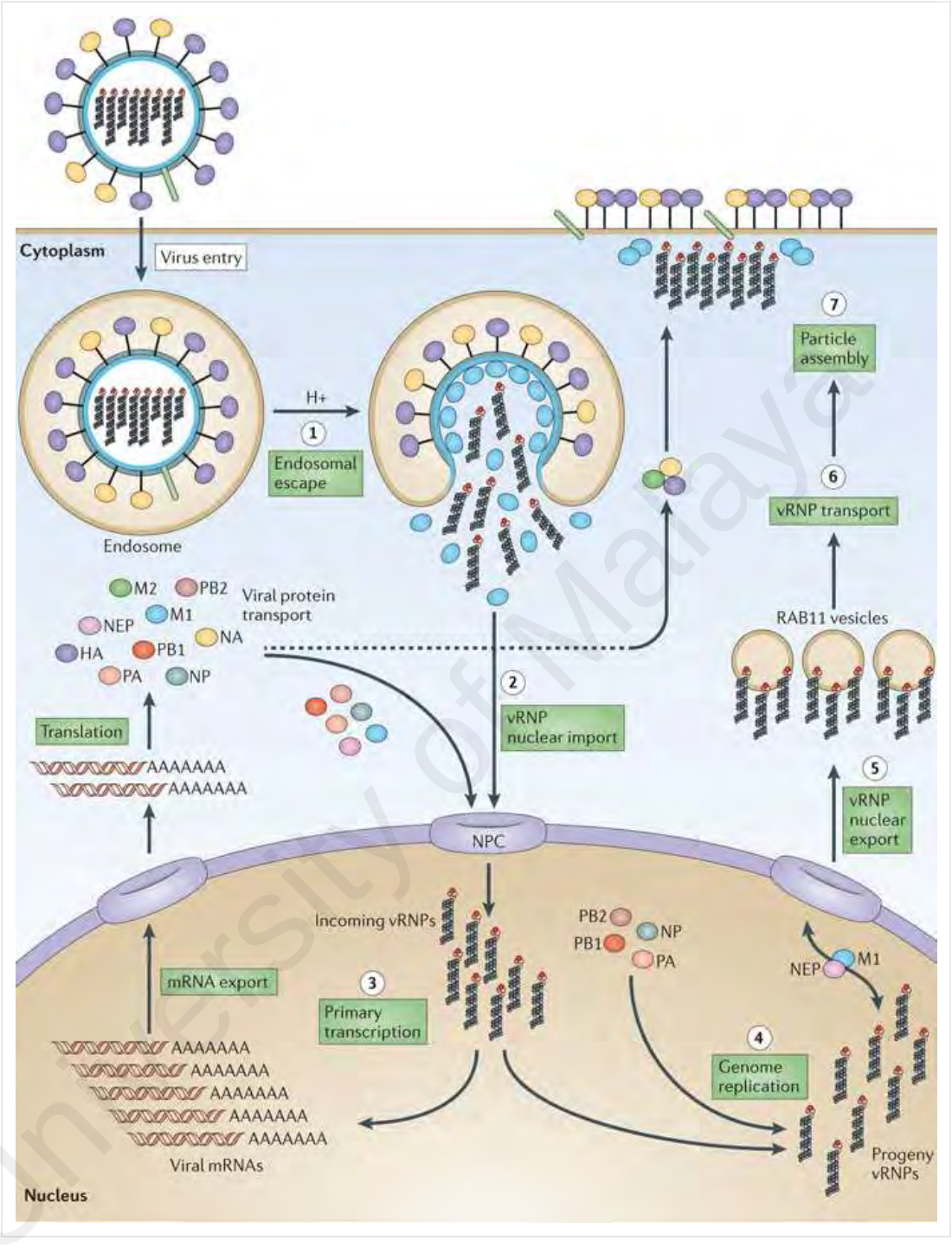

Figure 2.3: vRNPs in the IAV life cycle (Eisfeld et al., 2015).

2.4 Host Innate Immune Responses

Innate immune system, also known as the first line barrier, has no specificity towards a particular foreign microorganism. However, it is able to respond fast against a pathogen in the host body system. Influenza virus can be recognized by the innate immune system through pathogen-associated molecular patterns (PAMPs) via various pattern recognition receptors (PRRs) (Medzhitov, 2001). There are three main families of PRRs involved in IAV detection: the Toll like receptors (TLRs), the retinoic acid-inducible gene-I (RIG-I) and the nucleotide-binding oligomerization domain (NOD) like receptors (NLRs) (Iwasaki et al., 2014). The TLRs scan the extracellular and endosomal compartments while RIG-I and NLRs are involved in intracellular viral detection (Coates et al., 2015; Iwasaki et al., 2014).

2.5 Toll-Like Receptors

TLRs possess type I transmembrane receptors which consist of an extracellular leucine-rich repeat (LRR) domain and an intracellular Toll/IL-1 receptor (TIR) domain (Medzhitov, 2001). To date, there are eleven TLRs that can be described in human (Coates et al., 2015; Takeda et al., 2005). Among all, TLR 3 recognizes the double-stranded viral RNA when IAV replicates in epithelial cell, while TLR7 identifies the single-stranded IAV RNA (Goraya et al., 2015; Iwasaki et al., 2014) (Figure 2.4). When TLRs are triggered, either nuclear factor-κB (NF-κB) or interferon (IFN) regulatory factor 7 (IRF7) will be activated and stimulates the production of pro-inflammatory cytokines and type I IFN (IFN α and IFN β) to inhibit viral replication and promote antibody responses (Coates et al., 2015; Goraya et al., 2015; Iwasaki et al., 2014).

2.6 RIG-I

As a member of the RIG-like helicase receptor family, RIG-I has a crucial role in detecting influenza ssRNA during IAV replication in alveolar macrophages and epithelial cells (Goraya et al., 2015; Loo et al., 2008). RIG-I works by recognizing the 5'-triphosphate viral ssRNA produced during viral replication (Coates et al., 2015; Goraya et al., 2015; Iwasaki et al., 2014). Upon RIG-I activation by the viral RNA, ATP will be utilized by the helicase domain of RIG-I to initiate a series of conformational changes to free-up the caspase activation and recruitment domains (CARDs) to bind to the signalling adaptor mitochondrial antiviral signalling protein (MAVS) resulting in the activation of NF-κB pathway and the IFN signalling pathway (Iwasaki et al., 2014; Jiang et al., 2011) (Figure 2.4).

2.7 NLRs

All NLRs consist of a leucine-rich repeat (LRR) domain which functions as a ligand sensor and a negative regulator for NLR activation (Davis et al., 2011). NLRs possess an N-terminal effector domain which enables homotypic protein-protein interactions with adaptor proteins and enzymes such as procaspase-1 (Ting et al., 2008). NLR family also has a nucleotide-binding domain (NBD) for ATP-binding since energy is required during oligomerization of NLRs (Jacobs et al., 2012). During IAV infection, NLRP3 inflammasome will be activated and induces IL-1β production (Segovia et al., 2012). NOD2, one of the NLR proteins, will also be activated and lead to IFN-β production in cells and macrophages (Sabbah et al., 2009).

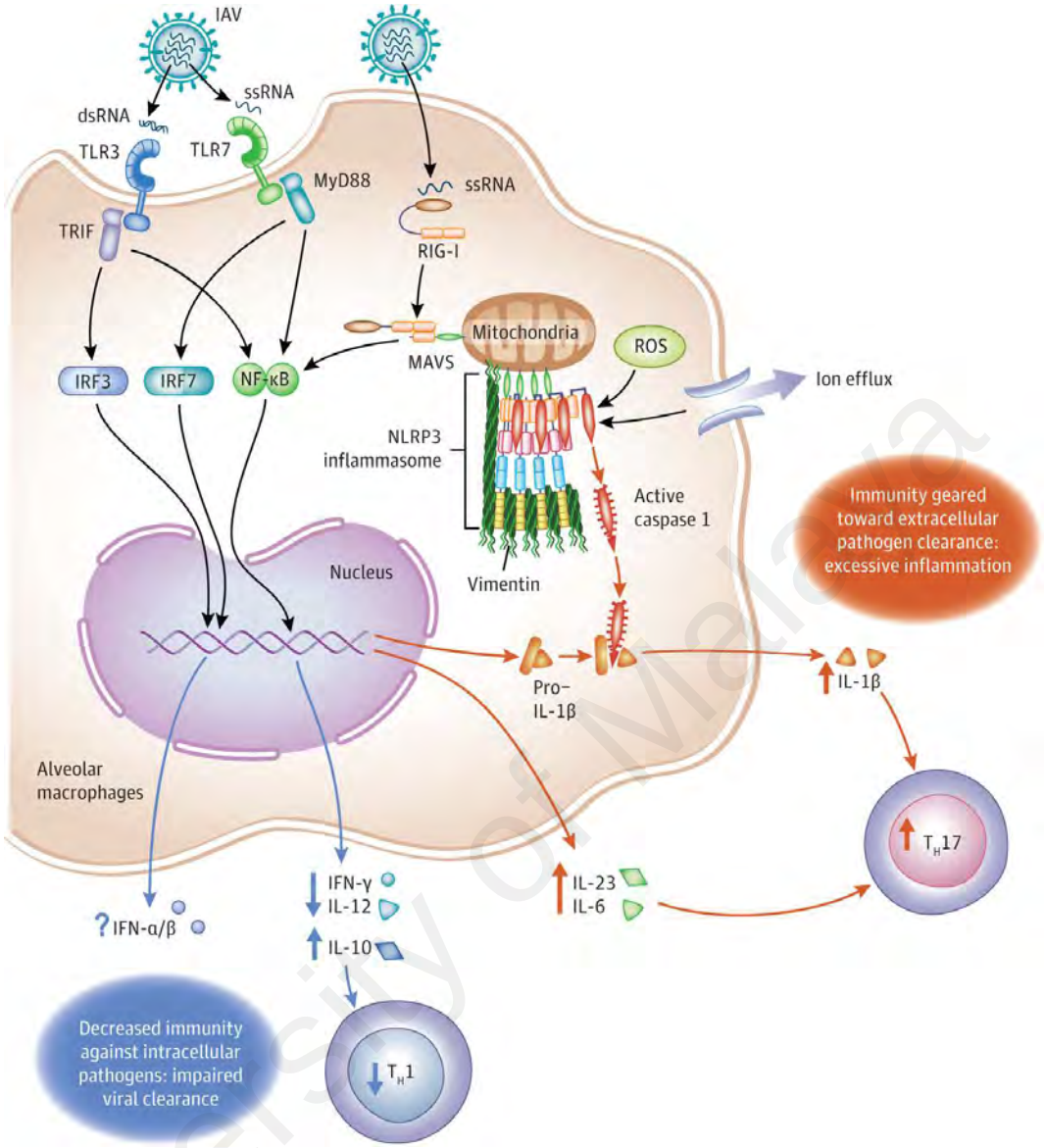

Figure 2.4: The innate immune response to IAV infection (Coates et al., 2015).

2.8 Therapeutic Drugs

Two types of therapeutic drugs are currently being used to treat influenza infections: the M2 ion channel blockers and NA inhibitors (Das et al., 2010). M2 ion channel blockers (such as amantadine and rimantadine) are less effective due to extensive resistance towards the amino acid substitutions in the transmembrane domain of M2 protein (Pielak et al., 2009). NA inhibitors (such as oseltamivir, also called as Tamiflu, and zanamivir or Relenza) prevent the release of newly synthesized viruses from the cells (Thorlund et al., 2011). However, with the progressive resistance of IAV towards

oseltamivir, combination of drugs becomes an attractive alternative to treat and control influenza (Belardo et al., 2015; Thorlund et al., 2011). For example, the combination of nitazoxanide (NTZ), which is a thiazolide, anti-infective against enteritis, and NA inhibitor (oseltamivir) are able to present a synergic treatment for influenza infection (Belardo et al., 2015).

2.9 Indole Derivatives

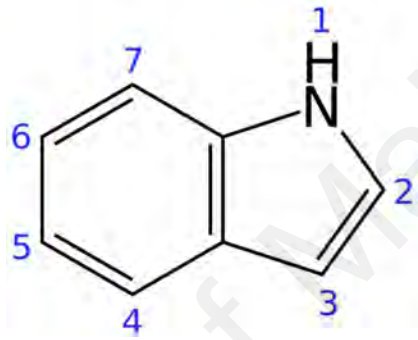

Figure 2.5: Structure of Indole (Source: https://en.wikipedia.org/wiki/Indole).

Indole derivatives carry an aromatic heterocyclic organic compound with a bicyclic structure, which consists of a six-membered ring fused to a five-membered nitrogen containing pyrrole ring (Figure 2.5). In general, indoles can be classified into two groups: isoprenoids and non-isoprenoids, depending on their biosynthesis (Dewick, 2002; Saxton, 1983).

Table 2.1: Classification of indoles.

Non-isoprenoids	Isoprenoids
• simple derivative of indole • simple derivatives of β-carboline • pyrroloindole alkaloids • indole-3-carbinole • indoleacetic • trypamines • carbazoles	• hemiterpenoids • monoterpenoids • strictosidine • catharanthine • vinca • yohimbine • strychnine • ellipticine

Indoles are the most ubiquitous component of biologically active natural products and possess a wide range of biological activities (Mehta et al., 2005). With unique characteristic of mimicking the structure of peptides and able to bind reversibly to enzymes (Zhang et al., 2015), indole derivatives remain to be a fascinating subject to be studied in both academia and industry. Studies found that indole derivatives possess some biological properties, such as anti-inflammatory (Ozdemir et al., 2015) and anti-microbial activities (Mehta et al., 2005; Olgen et al., 2008). Some indole compounds also exhibited a remarkable potential of antiviral activities against Human Immunodeficiency Virus (HIV) (Zhang et al., 2015), Herpes Simplex Virus (HSV) types 1 and 2, Flavivirus, Respiratory Syncytial Virus (RSV) (Giampieri et al., 2009), Coxsackie B virus (Xue et al., 2014) and Hepatitis C Virus (Han et al., 2016). Besides, some indole derivatives protect red blood cells and DNA against radical-induced oxidation (Zhao et al., 2009). Indoles can also act as an intercellular signal molecule to regulate bacteria physiology (Lee et al., 2010).

Thus, indole derivatives may possess a huge potential as antiviral drugs and play a vital role in controlling fast-spreading epidemics such as influenza A. Owing to the continuous evolution of major viral antigens that leads to drug resistance and low efficacy to treatment, a search for effective anti-influenza drug is extremely crucial for the society to handle the existing influenza pandemics as well as new pandemic strains.

CHAPTER 3: MATERIALS & METHODS

3.1 Cell Culture

A549-PB1 cells and HEK293T-PB1 cells were cultured in DMEM (GIBCO, USA) supplemented with 10 % fetal bovine serum (FBS) (GIBCO, USA), penicillin G (100 U/ml), and streptomycin (100 µg/ml) (GIBCO, USA). Cells were maintained at 37°C with 5 % CO_2 in a humidified incubator. Both A549-PB1 cells and HEK293T-PB1 cells (for viral amplification purpose) were sourced from Fred Hutchinson Cancer Research Center (USA).

3.2 Antibodies and Compounds

Antibodies against actin (I-19) (Santa Cruz Biotech), Hsp90α (Santa Cruz Biotech), p-IRF3 (Cell Signaling), p-STAT1 (Santa Cruz Biotech), PARP-1 (Santa Cruz Biotech) and NP (H16-L10-4R5, ATCC) were purchased from the respective commercial sources. Four compounds (source from Chemistry Department, University of Malaya) were dissolved in DMSO and DMSO was used as a mock treatment. The details of the compounds are included in Table 3.1.

Table 3.1: Details of compounds.

Compound No.	Chemical Formula	Molecular Weight (kDa)
525A	$C_{13}H_{12}ClNO_2$	250
526A	$C_{14}H_{15}NO_3$	245
527A	$C_{14}H_{12}F_3NO_3$	299
528A	$C_{13}H_{12}BrNO_2$	294

3.3 Cell Proliferation Assay

To obtain the working concentration of the four compounds, ten thousand of A549-PB1 cells were seeded in a 96-well plate and incubated overnight. Then, the cells were treated with and without the four compounds respectively at various concentrations and incubated for two days at 37˚C. Subsequently, 10 µl of 1 mg/ml 3-(4, 5-dimethylthiazol-2-yl)-2, 5-diphenyltetrazolium bromide (MTT) (Sigma, USA) was added to each well followed by 2 hours incubation at 37˚C in a CO_2 incubator. The medium was carefully discarded. Then, 100 µl of Dimethyl sulfoxide (DMSO) (Sigma, USA) was added to each well. After gently mixing to dissolve the formazan crystal formed, the absorbance was measured with a M200 PRO microplate reader (Tecan, Switzerland) at 540 nm wavelength. IC_{50} was calculated with GraphPad Prism 6. IC_{50} is the concentration where the compound kills 50 % of the cells.

3.4 Viral Amplification

PR8 strain IAV carrying *enhanced green fluorescent protein (*eGFP) in place of the PB1 gene (PR8-PB1flank-eGFP virus) (Figure 3.1) was amplified by infecting human embryonic kidney 293T cells that stably express PB1 protein (HEK239T-PB1 cells). Ten million of HEK293T-PB1 cells were seeded in 15 cm plate and incubated overnight. Prior to virus infection, HEK293T-PB1 cells were washed once with PBS and then changed with influenza growth media (RPMI supplemented with 0.2 % bovine serum albumin, 0.01 % heat-inactivated fetal bovine serum, 100 U/ml penicillin, 100 µg/ml streptomycin and 1 mM calcium chloride) (GIBCO, USA) containing 6 µg/ml TPCK-treated trypsin. After 24 hours, the supernatant was harvested and filtered using a 0.45 µm filter. The virus titer was later determined by FACS. The remaining IAV was stored at -80˚C refrigerator.

Figure 3.1: Non-replicative PR8 strain IAV carrying eGFP in place of the PB1 gene (Bloom et al., 2010; Wong et al. 2015).

3.5 Compound Screening for Antiviral Activity

For screening against IAV, ten thousand of A549-PB1 cells per well were seeded in a 96-well flat plate. After overnight incubation, cells were washed once with PBS (Sigma, USA) and then changed into influenza infection media containing 0.2 µg/ml TPCK-treated trypsin (Thermo Scientific, USA). Fifty micromolar (the working concentration as optimized previously) of each compound was added and incubated for four hours at 37˚C. PR8-PB1flank-eGFP Influenza A virus was then added at an MOI of 1.0. After eighteen hours, bright field (BF) and immunofluorescence images of the cells were photographed respectively using an Olympus IX73 inverted microscope at 200X final magnification (Olympus, Japan) and analyzed using Cellsens standard software (Olympus, Japan).

For screening against VSV, ten thousand of A549-PB1 cells per well were seeded in a 96-well flat plate. After overnight incubation, cells were washed once with PBS and then changed with influenza infection media containing 0.2 µg/ml TPCK-treated trypsin. Fifty micromolar of each compound was added and incubated for four hours at 37˚C. Vesicular stomatitis virus carrying a GFP (VSV-GFP) was added at an MOI of 1.0 for sixteen hours.

3.6 Virus Titering

Two hundred thousand of A549-PB1 cells were seeded in a 12-well plate with and without 75 µM of 526A for four hours followed by infecting the cells with PR8-PB1flank-eGFP Influenza A virus at an MOI of 0.75 in influenza growth media containing 6 µg/ml of TPCK-treated trypsin. Eighteen hours later, the supernatants were collected and filtered through 0.45 µm filters. The viruses in the collected supernatants were titered by infecting fresh A549-PB1 cells in influenza infection media containing 0.2 µg/ml of TPCK-treated trypsin. After 24 hours, cells were washed with PBS and fixed with 0.1 % formaldehyde (Thermo Scientific, USA) to inactivate the virus. Fixed cells were analyzed using MACSQuant Analyzer (Miltenyi Biotec, Germany) to quantify eGFP-positive cells. Data were further analyzed with FlowJo software. Total infectious virus particle (IP) was calculated based on the following formula: IP/ml = (% of the eGFP-positive cell) X (total cell number) / (total volume of supernatant used to infect the cells, in ml). One IP per cell was used when infecting cells at the MOI of 1.0.

3.7 Immunoblot Analysis

Two hundred thousand of A549-PB1 cells were seeded in a 12-well plate. After overnight incubation, culture media were removed, washed with PBS and changed into 1 ml of IAV infection media which containing 0.2 µg/ml TPCK-treated trypsin (Thermo Scientific, USA). Next, cells were pre-treated with and without 526A at various concentrations for four hours. IAV was added at an MOI of 1.0 for 12 hours. Whole cell lysate extracts were prepared from treated cells using a kinase lysis buffer (Table 3.2). After 30 minutes of on ice incubation, lysates were collected by centrifugation at 15 000 rpm, 4˚C for 10 minutes. The concentration of proteins was quantified using Bradford assay.

Table 3.2: Kinase lysis buffer recipe.

Chemical	Concentration
Tris pH 7.5 (Thermo Scientific, USA)	20 mM
Sodium chloride (Thermo Scientific, USA)	120 mM
Glycerol (Thermo Scientific, USA)	10 %
Triton X-100 (Sigma, USA)	1 %
β-glycerophosphate (Thermo Scientific, USA)	25 mM
Sodium orthovanadate (Sigma, USA)	1 mM
Dithiothreitol (DTT) (Sigma, USA)	1 mM
Phenylmethanesulfonylfluoride (PMSF) (Sigma, USA)	1 mM

3.7.1 Bradford Protein Assay

The concentration of proteins to be used for immunoblotting was measured using Bradford assay. Bradford assay was performed by adding 1 µl of the protein lysates and Bovine Serum Albumin (BioRad, USA) standards to 500 µl of 1X Bradford reagent respectively (BioRad, USA). Two hundred microliter of each mixed solution (both protein samples and standards) was subsequently transferred into a 96-well plate to measure the absorbance using a M200 PRO microplate reader at 595 nm wavelength. The standard curve was constructed by serial dilution of 1 mg/mL of BSA (Sigma, USA). From the equation of the standard curve, the concentration of protein samples was calculated.

3.7.2 Sodium Dodecyl Sulfate Polyacrylamide Gel Electrophoresis (SDS-PAGE)

Based on the calculation from Bradford assay, the protein lysates mixed with 5X sample buffer (0.5 M Tris pH 6.8, 20 % SDS, 80 % glycerol and 5 % Bromophenol Blue (filtered)) were boiled at 95 °C for ten minutes to denature the folded protein.

After boiling, the protein samples were quick spun at 16,800 rpm for one minute before loading into the SDS gel containing 5 % acrylamide stacking gel and 10 % acrylamide resolving gel. The samples were run at 180 V for 45 minutes using a mini gel tank filled with 1X running buffer (Dilution from 10 X running buffer consists of 0.025 M Tris pH 8.5, 1.92 M Glycine, 1 % SDS).

3.7.3 Western Blotting

After SDS-PAGE was run, the proteins in the gel were transferred onto methanol (Emsure, Germany)-activated polyvinylidene difluoride (PVDF) membrane (Millipore, USA) in 1X transfer buffer (0.25 M Tris, 1.92 M Glycine) at 250 mA for 75 minutes. After transfer, membrane was blocked with 3 % of skim milk in 100 ml of TBST (Tris-buffered saline with 0.05 % of tween 20) for one hour. After blocking, the membranes were blot with respective primary antibodies, such as anti-NP, anti-actin, anti p-IRF3, anti p-STAT1 and anti-HSP90α antibodies. After overnight incubation at 4 °C, primary antibodies were removed and the membranes were washed three times using TBST with five minutes interval each. Secondary horseradish peroxidase (HRP)-conjugated antibodies were then added and incubated at room temperature for an hour.

Next, the membranes were washed three times using TBST with five minutes interval each. Then, chemiluminescent substrate (Thermo Scientific, USA) working solution was prepared by mixing equal volumes of the peroxide solution and the enhanced luminol solution. Finally, the substrate was added onto the membranes and viewed under a Bio-Rad ChemiDoc™ XRS System. Images were taken and processed using BioRad Image Lab version 5.0 and Adobe Photoshop CS4.

3.8 Quantitative Polymerase Chain Reaction (RT-qPCR)

Two hundred thousand of A549-PB1 cells were seeded in a 12-well plate. After overnight incubation, culture media were changed into IAV infection media containing 0.2 μg/ml TPCK-treated trypsin (Thermo Scientific, USA) and pre-treated with and without 75 μM 526A for four hours. IAV virus was added at an MOI of 1.0 for twelve hours. Total RNAs were isolated using the Thermo Scientific GeneJET RNA Purification Kit. Complementary DNAs were synthesized using M-MuLV reverse transcriptase (New England BioLabs, USA), Random Hexamers (Invitrogen, USA), dNTPs (Thermoscientific), and RNase inhibitor (NEB). Quantitative PCR was performed with 2X KAPA SYBR Fast qPCR Master Mix (Thermo Scientific, USA) on a Bio-Rad Connect Real-Time PCR System to measure the expression of IAV vRNAs, mRNAs, interferon stimulated genes and cytokines (Table 3.3). All data were normalized to *L32*.

Table 3.3: List of primer sequences used in RT-qPCR assays.

Genes	Primer Sequence 5' – 3'
L32 Forward	AGCTCCCAAAAATAGACGCAC
L32 Reverse	TTCATAGCAGTAGGCACAAAGG
eGFP Forward	AGATCCGCCACAACATCGAG
eGFP Reverse	TCTCGTTGGGGTCTTTGCTC
M1 Forward	AAGACCAATCCTGTCACCTCTGA
M1 Reverse	CAAAGCGTCTACGCTGCAGTCC
NS1 Forward	CTTCGCCGAGATCAGAAATC
NS1 Reverse	TGGACCATTCCCTTGACATT
PR8-NP Forward	ACGGCTGGTCTGACTCACAT
PR8-NP Reverse	TCCATTCCGGTGCGAACAAG
SDHA Forward	TGGGAACAAGAGGGCATCTG
SDHA Reverse	CCACCACTGCATCAAATTCATG
β-actin Forward	CGTCTTCCCCTCCATCG
β-actin Reverse	CTCGTTAATGTCACGCAC
18S Forward	GTAACCCGTTGAACCCCATT
18S Reverse	CCATCCAATCGGTAGTAGCG
IFNβ Forward	ACTGCCTCAAGGACAGGATG
IFNβ Reverse	AGCCAGGAGGTTCTCAACAA
IFIT2 Forward	GCGTGAAGAAGGTGAAGAGG
IFIT2 Reverse	GCAGGTAGGCATTGTTTGGT
IP10 Forward	GACCAATGATGGTCACCAAA
IP10 Reverse	GCAGGGTCAGAACATCCACT

Table 3.3, continued.

Genes	Primer Sequence 5' – 3'
IL6 Forward	TACCCCCAGGAGAAGATTCC
IL6 Reverse	TTTTCTGCCAGTGCCTCTTT
TNFα Forward	GCCCAGGCAGTCAGATCATCT
TNFα Reverse	TTGAGGGTTTGCTACAACATGG

3.9 Cell Transfection

For poly I:C transfection, four hundred thousand of A549-PB1 cells were seeded in a 12-well plate using Opti-MEM® 1X (Thermo Scientific, USA) and pre-treated with and without 75 μM 526A. After four hours, 100 ng of Poly I:C (Tocris Bioscience, UK) was transfected into the A549-PB1 cells using X-tremeGENE HP DNA transfection (Roche, Switzerland). After six hours, total RNAs were isolated and complementary DNAs were synthesized. Quantitative PCR was performed using a Bio-Rad Connect Real-Time PCR System to measure the expression of interferon stimulated genes. All data were normalized to *L32*.

For PAMer-Cy3 (sequence: 5' CCTCGCCAAGGGCCATCCTGTGCGCCA-CY 3') transfection, four hundred thousand of A549-PB1 cells were seeded in a 12-well plate using Opti-MEM® 1X (Thermo Scientific) and pre-treated with or without 75 μM 526A. After four hours, 20 μM of Pamer-Cy3 was transfected into the A549-PB1 cells using X-tremeGENE HP DNA transfection (Roche). After twelve hours, cells were washed with PBS and fixed with 0.1 % formaldehyde. Fixed cells were analyzed using a MACSQuant Analyzer (Miltenyi Biotec, Germany) to quantify Pamer-Cy3 positive cells. Data were further analyzed with FlowJo software.

3.10 Statistical Analysis

Data were analysed with Microsoft Excel and presented as mean ± SD. Data are representative of two independent experiments. Statistical significance was assessed using two-tailed Student's *t*-test.

CHAPTER 4: RESULTS

4.1 Screening of four novel synthetic indole derivatives for antiviral property.

Four new synthetic indole derivatives (Table 3.1 and Figure 4.1a) were synthesized by Prof. Hapipah's group from the Chemistry Department, University of Malaya. In this study, the indole derivatives were tested for antiviral activity using a cell-based screening system for IAV replication inhibitors (Wong et al., 2015). A non-replicative PR8 strain IAV carrying eGFP in place of the PB1 gene (PR8-PB1flank-eGFP) was used to infect A549 cells that stably express PB1 protein (A549-PB1). Upon PR8-PB1flank-eGFP viral infection and replication, infected A549-PB1 cells will express the eGFP reporter. Prior to studying the four indole derivatives on IAV infection, the cytotoxic effects of each compound were determined in A549-PB1 cells using the MTT assay. After two days of incubation, all compounds were found to be non-toxic at the concentration below 100 μM (Figure 4.1b) with the IC_{50} of 442 μM for 525A, 266 μM for 526A and 341 μM for 528A while the IC_{50} value for 527A was too high. (Figure 4.1b and Appendix A).

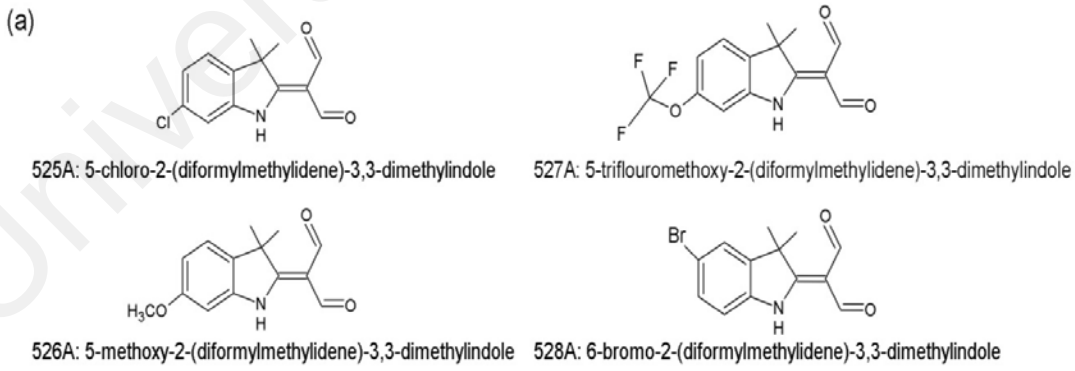

Figure 4.1: Screening of the four novel synthetic indole derivatives for antiviral property.

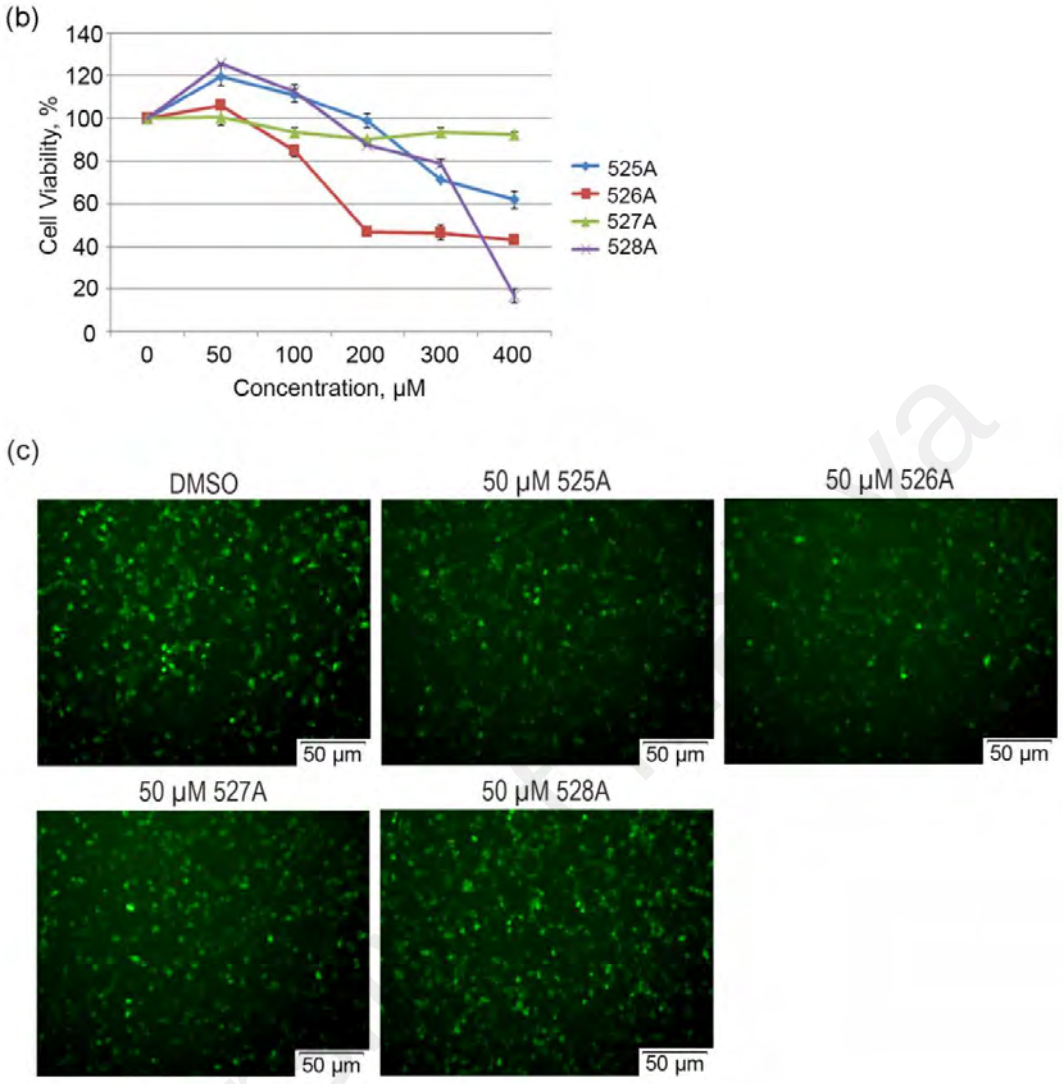

Figure 4.1, continued.
(a) Chemical structures and chemical names of 525A, 526A, 527A and 528A. (b) A549-PB1 cells were seeded in a 96-well plate and pre-treated with various concentrations of the four compounds (525A, 526A, 527A and 528A) for two days. Cells viability was measured with a MTT assay. Error bars represent the variation range of triplicate experiments. (c) A549-PB1 cells were seeded in a 96-well plate and pre-treated with the four compounds at 50 μM for four hours followed by PR8-PB1flank-eGFP IAV infection at a MOI of 1.0 for eighteen hours. Fluorescence microscopy images were taken using an Olympus IX73 inverted microscope at 200x final magnification and photographed using an Olympus DP73 digital camera with Cellsens standard software.

To screen if any of the indole derivatives possesses antiviral property, the A549-PB1 cells were pretreated with 50 μM of the indole derivatives for four hours and infected the cells with PR8-PB1flank-eGFP IAV at a multiplicity of infection (MOI) of 1.0. No obvious reduction of eGFP-positive cells was found on both 527A and 528A-treated cells, and slightly less eGFP-positive cells was observed in 525A-treated cells (Figure 4.1c and Appendix C). Interestingly, 526A pretreatment led to a moderate reduction of eGFP-positive cells (Figure 4.1c and Appendix C). The antiviral activity of 526A was not due to their cytotoxic effect as cell proliferation was unaffected at 50 μM (Figure 4.1b) and treated cells displayed normal morphology (Appendix B). Thus, 526A was selected for further testing.

To determine if all four indole derivatives also exert antiviral activity against other viruses, A549-PB1 cells were pretreated with each derivative for four hours and infected the cells with a vesicular stomatitis virus carrying a GFP (VSV-GFP) at a MOI of 1.0. More than 90 % of GFP-positive cells were observed in DMSO-treated A549-PB1 cells while four compounds possess different levels reduction of GFP-positive cells (Appendix D). Among the four, 525A showed the highest reduction of GFP-positive cells (Appendix D). These results suggest that all four indole derivatives protect cells from VSV-GFP infection to varying degrees.

4.2 526A suppresses IAV replication.

To investigate whether 526A affects the replication of IAV, the IAV polymerase activity was studied by measuring the expression of both negative strand vRNAs and positive strand viral mRNA using RT-qPCR. A549-PB1 cells were pre-treated with 75 μM of 526A for four hours followed by PR8-PB1flank-eGFP IAV infection at a MOI of 1.0 for various time points up to twenty-four hours. Seventy five micromolar of 526A was used to treat the A549-PB1 cells here and for the later experiments because it gives more significant antiviral activity with negligible cytotoxicity (Figure 4.1b) compared to 50 μM 526A (data not shown). At the first-hour post-IAV infection, no significant difference in the levels of vRNAs including NP, NS1, eGFP, and M1 were detected between DMSO- and 526A-treated cells (Figure 4.2a). During the early phase of IAV infection, incoming IAV genomes are the major source of vRNAs in infected cells. Thus the result suggested that DMSO- and 526A-treated cells had similar IAV infection rate and 526A did not block the entry of IAV. The levels of vRNAs increased dramatically at six hours post-infection indicating active replication of IAV. However, the expression of vRNAs was reduced at six hours post-infection in the 526A-treated A549-PB1 cells implies that 526A inhibited the replication of IAV (Figure 4.2a). Similarly, the transcription of NP, NS1, eGFP, and M1 was significantly lower in the presence of 526A (Figure 4.2a). To rule out the reduction of the transcription of viral mRNAs observed in 526A-treated A549-PB1 cells is due to the defect in host cell general transcription machinery or the RNA processing by 526A treatment, the expression levels of three housekeeping genes (SDHA, β-actin and 18S) in both the DMSO-treated and 526A-treated samples were quantified (Appendix E). No significant difference in the expression level of all three housekeeping genes was observed, suggesting that 526A does not inhibit the host cell general transcription machinery or RNA processing.

To investigate whether the influenza protein level was affected by 526A, immunoblotting on whole cell extracts with an antibody against NP protein was performed. The NP protein was readily detected in DMSO-treated cells twelve hours post-IAV infection (Figure 4.2b and Appendix F) but was reduced significantly in 526A-treated A549-PB1 cells. This finding indicated that 526A reduces viral protein synthesis.

To determine whether 526A inhibits viral replication, the viral titer in the culture media collected from PR8-PB1flank-eGFP virus-infected A549-PB1 cells pre-treated with or without 526A was measured. The infected cells were quantified with FACS by sorting the viral-infected, eGFP-positive cells (Figure 4.2c). Consistent with the microscopy analysis (Figure 4.1c), 526A-treated A549-PB1 cells showed a 24 % reduction of total eGFP-positive cells compared to DMSO-treated control A549-PB1 cells (Figure 4.2c, 4.2d, and 4.2e left panel). Among the eGFP-positive cells, there were about 5 % of 526A-treated cells showed the high expression level of eGFP while about 40 % high eGFP-expressing cells were observed in the DMSO-treated sample (Figure 4.2c). Importantly, there was an 18 fold reduction of new virus generated in the presence of 526A (Figure 4.2e, right panel). Together, these results imply that 526A inhibits IAV replication.

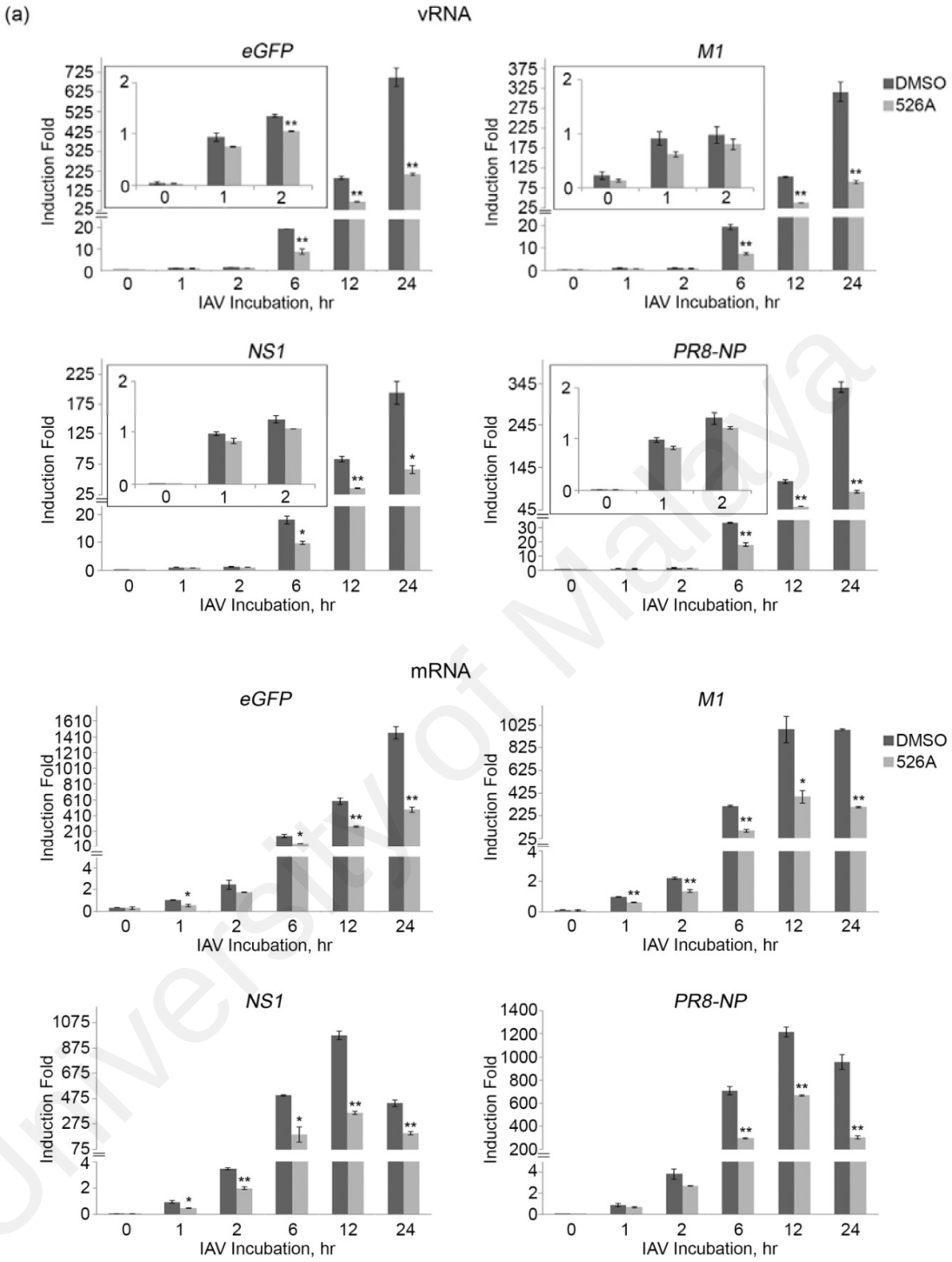

Figure 4.2: 526A suppresses IAV replication.

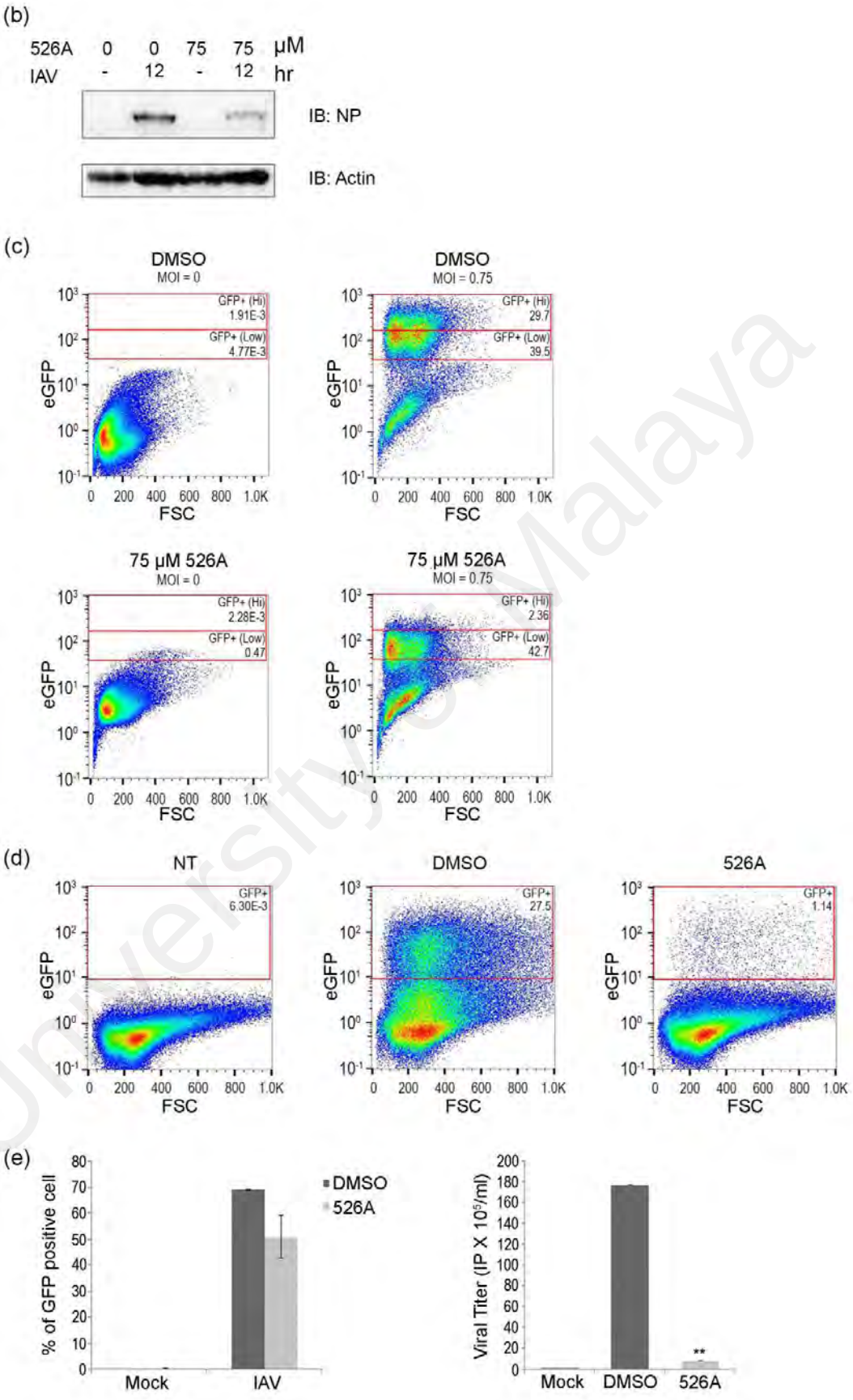

Figure 4.2, continued.

(a) A549-PB1 cells were pre-treated with or without 75 μM 526A for four hours and subjected to PR8-PB1flank-eGFP IAV infection at an MOI of 1.0 for the indicated time points. The expression of M1, NS1, PR8-NP and eGFP from both IAV negative-strand vRNA and positive-strand mRNA was measured with RT-qPCR. Error bars represent the variation range of duplicate experiments. (b) A549-PB1 cells were treated with or without 75 μM 526A for four hours and subjected to PR8-PB1flank-eGFP IAV infection at a MOI of 1.0 for twelve hours. The whole cell extracts were collected and subjected to immunoblotting with antibodies against NP and actin. (c) A549-PB1 cells were pre-treated with or without 75 μM 526A for four hours and subjected to PR8-PB1flank-eGFP IAV infection at a MOI of 0.75 for eighteen hours. Cells were washed and fixed with 0.1 % formaldehyde before titering with FACS. (d) A549-PB1 cells were infected with the harvested supernatant in Figure 4.2c and subjected to a viral titering assay using FACS. NT: non-treated sample. (e) The left panel shows the percentage of GFP-positive cells upon primary IAV infection in A549-PB1 cells while the right panel shows the viral titering of secondary IAV infection from the harvested viral supernatant. Error bars represent the variation range of duplicate experiments. IP: infectious viral particle. Student's t-test: *, $p < 0.05$; **, $p < 0.01$.

4.3 526A represses IAV-induced interferon stimulated genes (ISGs) and cytokine expression

In response to viral infection, the host cells will mount a type I interferon response to produce cytokines to eliminate the viral infection. To determine whether 526A suppresses IAV infection by amplifying the host cell antiviral responses, the expression of ISGs and cytokines in IAV-infected A549-PB1 cells pre-treated with or without 75 μM of 526A were quantified. The A549-PB1 cells were infected with PR8-PB1flank-eGFP IAV at a MOI of 1.0 for twelve hours and measured the gene expression with RT-qPCR (Table 3.3). All of the ISGs and cytokine genes, including *IFNβ*, *IFIT2*, *IL6*, and *IP10* were induced upon PR8-PB1flank-eGFP IAV infection in DMSO-treated A549-PB1 cells (Figure 4.3). On the other hand, viral-induced the expression of *IFNβ*, *IFIT2*, *IL6* and *IP10* were greatly reduced in 526A-treated A549-PB1 cells (Figure 4.3). These results indicate that 526A does not protect the host cells from IAV infection by enhancing the antiviral response.

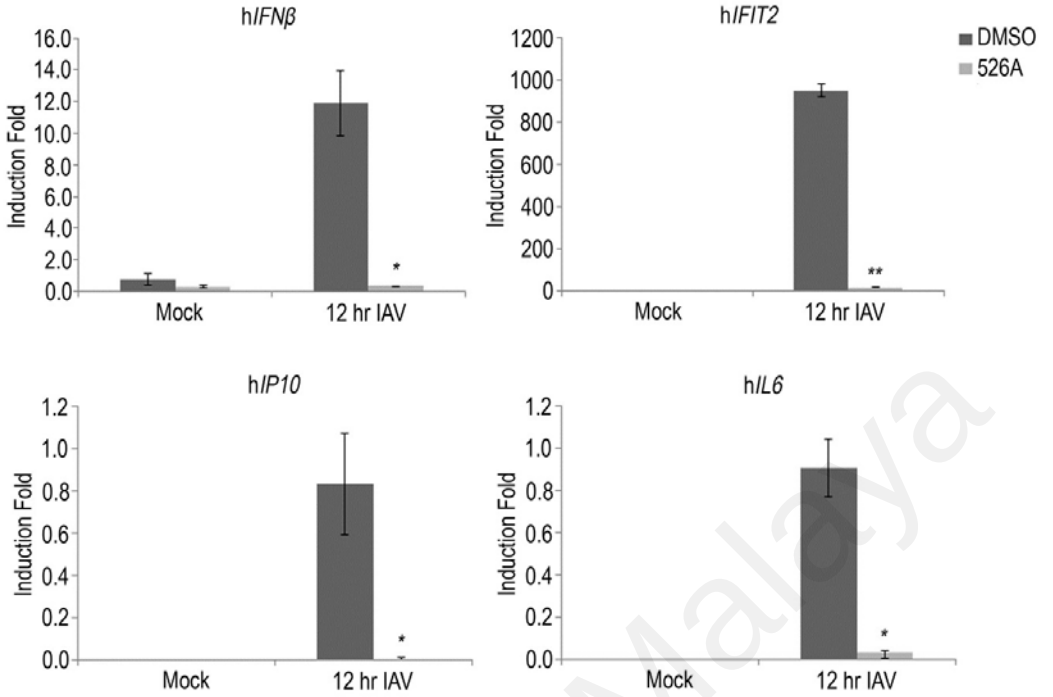

Figure 4.3: 526A represses IAV-induced interferon stimulated genes (ISGs) and cytokine expression.
A549-PB1 cells were pre-treated with or without 75 μM 526A for four hours and subjected to PR8-PB1flank-eGFP IAV infection at an MOI of 1.0 for twelve hours. The expression of *IFNβ*, *IFIT2*, *IP10* and *IL6* was measured with RT-qPCR (Table 3.3). Error bars represent the variation range of duplicate experiments. Student's t-test: *, $p < 0.05$; **, $p < 0.01$.

4.4 526A inhibits IAV-induced IRF3 and STAT1 activation.

IRF3 pathway plays a crucial role in regulating the production of virus-induced ISGs and cytokines. Following RNA virus infection, IRF3 is activated, which, in turn, rapidly induce and activates the IFN-mediated transcription factor complex ISGF3, consisting of STAT1, STAT2 and IRF9 to produce ISGs and cytokines (Trinchieri, 2010). To determine whether 526A inhibits IAV-induced IRF3 and STAT1 activation, the phosphorylation of IRF3 (p-IRF3) and STAT1 (p-STAT1), a biochemical hallmark of IRF3 and STAT1 activation were measured respectively, in post viral-infected A549-PB1 cells with and without 526A treatment. 526A was shown to inhibit the activation of IRF3 in a dosage-dependent manner (Figure 4.4, middle panel and Appendix G). IAV-induced phosphorylation of IRF3 was abolished when the A549-PB1 cells were pre-treated with 75 μM of 526A. Similarly, IAV-induced phosphorylation of STAT1 was decreased in the presence of 526A (Figure 4.4, bottom panel and Appendix G). These results indicate that 526A inhibits IAV-induced activation of IRF3 and STAT1.

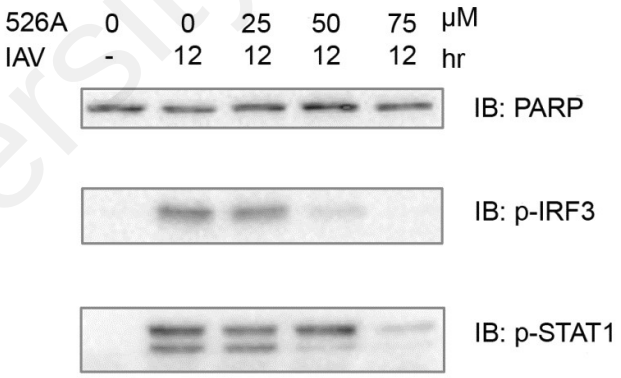

Figure 4.4: 526A inhibits IAV-induced IRF3 and STAT1 activation.
The A549-PB1 cells were treated with various concentrations of 526A as indicated for four hours followed by PR8-PB1flank-eGFP IAV infection at an MOI of 1.0 for twelve hours. Whole cell extracts were prepared and immunoblotted with antibodies against PARP, p-IRF3 and p-STAT1. PARP acts as a loading control.

4.5 526A affects detection of viral RNA by RIG-I pathway.

Retinoic-acid-inducible protein 1 (RIG-I) is a key sensor of RNA virus infection (including *orthomyxovirus*) and activates antiviral responses via induction of interferons (Goraya et al., 2015; Loo et al., 2008). The results showed that 526A blocked the viral replication (Figure 4.2), virus-induced activation of IRF3 and STAT1 (Figure 4.4 and Appendix G), and thus the IAV-induced induction of ISGs and cytokines (Figure 4.3). To test if 526A inhibits IAV-induced ISGs and cytokines production by blocking the RIG-I signaling pathway or simply through inhibiting the replication of IAV, the expression of ISGs and cytokines in A549-PB1 cells transfected with polyinosinic-polyctidylic acid (poly I:C), which is a synthetic analog of double-stranded RNA (dsRNA), in the presence or absence of 526A were measured. It was observed that transfecting DMSO-treated A549-PB1 cells with poly I:C induced the expression of *IFNβ, IFIT2, IL6* and *TNFα*, while no expression was detected if poly I:C was added directly to culture media (Figure 4.5a, Table 3.3). Interestingly, 526A moderately inhibited poly I:C-induced expression of *IFNβ* and *TNFα*, and inhibited the expression of *IFIT2* and *IL6* by 70-80 % (Figure 4.5a).

To rule out the possibility that 526A affects the transfection efficiency, the experiment was also mimicked by transfecting PAMer-Cy3 in A549-PB1 cells with and without 526A and measured the PAMer-Cy3 positive cells with FACs (Figure 4.5b). The percentage of PAMer-Cy3 positive cells was similar between DMSO- and 526A-treated A549-PB1 cells (Figure 4.5b). These results suggest that 526A treatment alone might partially block the RIG-I pathway.

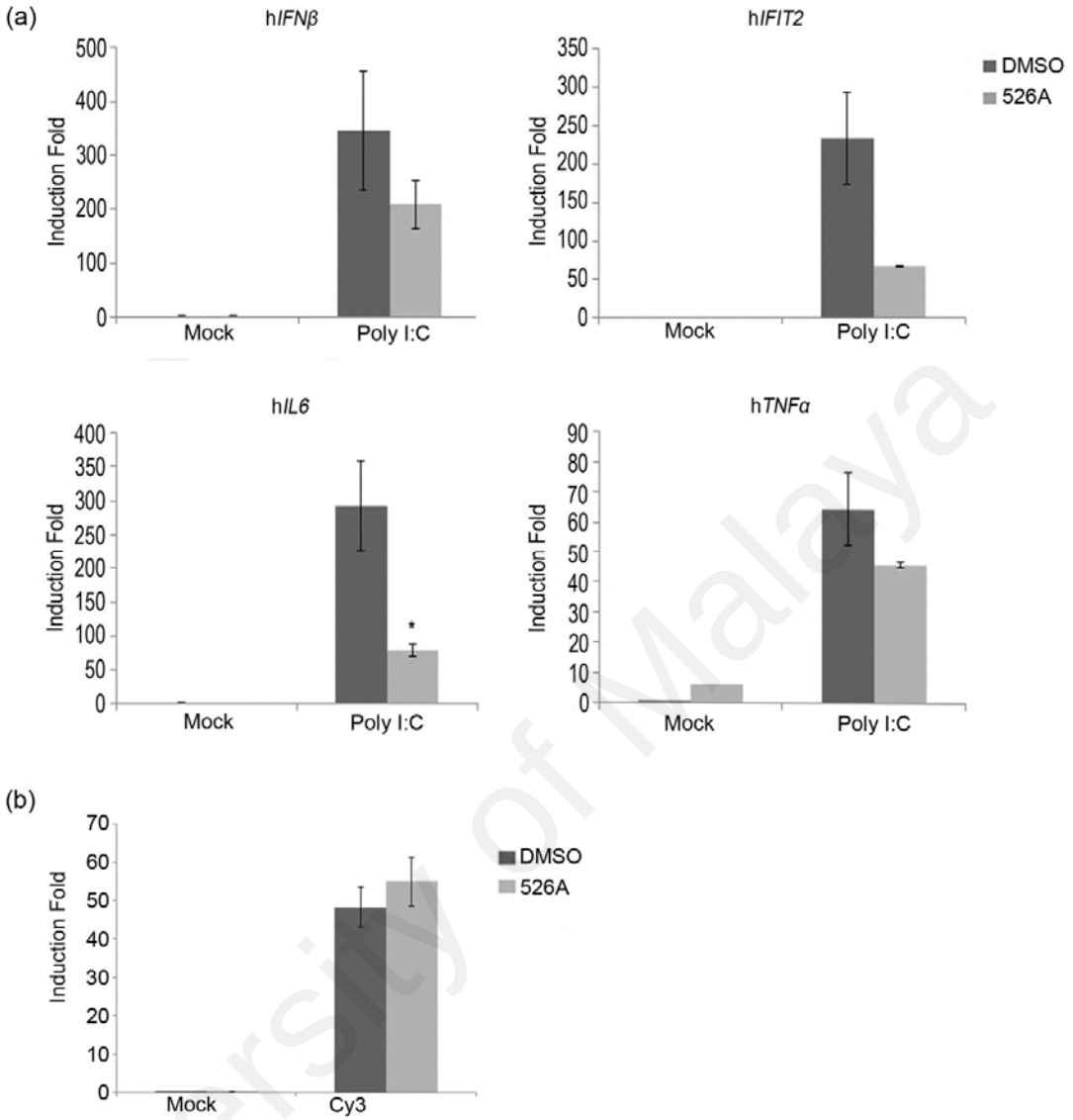

Figure 4.5: 526A affects detection of viral RNA by RIG-I pathway.
(a) A549-PB1 cells were pre-treated with or without 75 μM 526A for four hours. One hundred nanograms of poly I:C was transfected into the A549-PB1 cells using X-tremeGENE transfection method or added directly into the culture media without transfection (mock) for six hours. The expression of *IFNβ*, *IFIT2*, *IL6* and *TNFα* were measured with RT-qPCR. (b) A549-PB1 cells were pre-treated with or without 75 μM 526A for four hours. Twenty micromolar of PAMer-Cy3 was transfected into the A549-PB1 cells for twelve hours using X-tremeGENE transfection method. The signal of PAMer-Cy3 was measured using FACS. Error bars represent the variation range of duplicate experiments. Student's t-test: *, $p < 0.05$.

CHAPTER 5: DISCUSSION

Among all pathogens, RNA viruses impose a particular challenge due to their ability to evolve rapidly. Even though there are quite a number of drugs available in the market (eg. Amantadine) to counter act on the seasonal influenza virus, resistance to the drugs is constantly emerging (Belardo et al., 2015; Thorlund et al., 2011). Hence, there is an urgent need to develop new antiviral drugs against RNA viruses. Indole derivatives are the most ubiquitous components that exhibit various antiviral activities (Han et al., 2016; Zhang et al., 2015). They are also one of the favourite study subjects by researchers worldwide. Four novel indole derivatives were synthesized by the Chemistry Department, University of Malaya and their effects on influenza A virus were studied in this project.

A relatively quick and safe cell-based screening system for anti-IAV was adopted using a non-replicative PR8 strain carrying an eGFP in place of the PB1 gene (Bloom et al., 2010; Wong et al., 2015). It is a convenient and easy screening assay compared to the standard plaque assay which is time consuming and more laborious. Upon infection on A549 cells that stably express the PB1 protein, the cells will express the eGFP that can be quantitated by various methods (e.g. using fluorescent microscope, fluorescent microplate reader, etc). In all cases, the fluorescence correlates very well with the amount of PR8-PB1 flank-eGFP virus I used for infection.

Prior to data collection, sufficient IAV (stored at -80˚C) was amplified and the cell-based IAV screening assay was optimized. The MTT assays were performed to determine the working concentration of the compounds. All four compounds were found to be non-toxic at the concentration below 100 μM (Figure 4.1b). Through the screening process, all four compounds (525A, 526A, 527A and 528A) were demonstrated to possess different degrees of antiviral activity against IAVs and VSVs in which 526A was selected for further study due to its potent antiviral property (Figure

4.1c and Appendix D). These differences were expected because chemical modifications to the different sites of indole will certainly produce different characteristics such as the effect on different viruses.

IAV infection in a host cell can be interfered via multiple ways, including by inhibiting the entry of IAV, the release of vRNA, the entry of vRNA into the nucleus, restricting the viral genome replication or by blocking the budding of the newly synthesized virus (Samji, 2009). Thus, 526A was studied on its effect towards these multiple aspects. Based on the findings, 526A suppresses the transcription of IAV vRNAs and reduced the expression of IAV nucleoprotein (Figure 4.2) upon 526A treatment. However, similar amount of vRNAs were detected regardless in the presence or absence of 526A (Figure 4.2a) at the early phase of IAV infection, while vRNAs or their transcripts were significantly lower in the presence of 526A at the later stages of IAV infection. These findings suggest that 526A blocks the replication of IAV at a step after the entry of IAV.

Normally, type I interferon will be activated upon viral infection to restrict initial viral replication before mounting the humoral immunity system (Trinchieri, 2010). Therefore, the response of type I interferon towards IAV was studied in the presence or absence of 526A. Interestingly, 526A was found to suppress the IAV-induced expression of ISGs and cytokines (Figure 4.3). To further validate the result, the IRF3 and STAT1 activation were studied. From the data, 526A also represses the virus-induced activation of IRF3 and STAT1 (Figure 4.4 and Appendix G). These results suggest that 526A protects the host cells from IAV infection but unexpectedly, not through enhancing type I interferon response in the host cells.

Both toll-like receptors (TLRs) and the cytosolic RIG-I-like receptors (RLRs) are the first lines of defence that have been implicated in the induction of IFNs by influenza viruses (Killip et al., 2015). Since TLR7/8 is absent in the A549-PB1 cells used in this

study (Tissari et al., 2005), therefore detection of IAV would be mediated primarily through the RIG-I pathway which recognizes viral 5'ppp or 5'pp RNA in the cytosol (Goubau et al., 2014; Killip et al., 2015; Rehwinkel et al., 2010). The fact that 526A inhibits the ISGs expression upon poly I:C treatment (Figure 4.5a), albeit with a lesser degree compare to IAV-induced expression of ISGs (Figure 4.3) but not the host cell's general transcription machinery and RNA processing (Appendix E), further suggests that 526A may also directly inhibit the activation of RIG-I pathway.

Although A549-PB1 cells express Melanoma Differentiation-Associated protein 5 (MDA5) and protein kinase RNA-activated (PKR) (Pham et al., 2016), further experiments would be needed to investigate if 526A target those pathways. However, it is known that PKR is dispensable for IAV induced IFNβ production (Versteeg et al., 2011).

5.1 Limitations

The screening of compounds on anti-IAV property requires a large pool of candidate compounds because the chances for a potential synthetic compound to possess the anti-IAV effect can be very small. In this study, the optimization the TPCK-trypsin concentration and the HEK293T cell number to amplify the IAV stock has stretched the duration of this study. The cell number will determine how much starting IAV to be used and also the incubation time. In addition to that, the storage of the amplified IAV needs to be optimised as the stability of virus can gradually decreased upon time. Regular freeze-thaw cycles may have affected the activity of IAV too. Therefore, amplified IAV should be stored in small aliquots in -80˚C temperature, with DMSO.

5.2 Future Studies

Future studies will be directed towards the investigation on the detailed mechanism of how 526A elicits an antiviral response. To expand beyond *in vitro* model, animal study should be conducted to study the efficacy of the indole compound *in vivo* against IAV. Animal studies allow us to know their reaction towards 526A, under or without stress (IAV infected) condition. The findings from these future studies will lead to a better understanding on how 526A works and the development of a novel therapeutic target to combat IAV and potentially other viral infections.

CHAPTER 6: CONCLUSION

The indole derivative 526A is a promising compound and was selected for further testing of its biological activity. Pre-treating adenocarcinomic human alveolar basal epithelial cells with 526A protects the cells from IAV infection. Furthermore, 526A inhibits IAV replication by mainly inhibiting the expression of IAV genes and proteins. Interestingly, 526A also suppresses the activation of IRF3 and STAT1 in host cells and thus represses the production of type I interferon response and cytokines in IAV-infected cells by partially inhibiting the activation of RIG-I pathway. Taken together, these results suggest that 526A may be a potential anti-influenza A virus agent.

REFERENCES

Belardo, G., Cenciarelli, O., La Frazia, S., Rossignol, J. F., & Santoro, M. G. (2015). Synergistic effect of nitazoxanide with neuraminidase inhibitors against influenza A viruses in vitro. *Antimicrobial Agents and Chemotherapy, 59*(2), 1061-1069.

Bloom, J. D., Gong, L. I., & Baltimore, D. (2010). Permissive secondary mutations enable the evolution of influenza Oseltamivir resistance. *Science, 328*(5983), 1272.

Coates, B. M., Staricha, K. L., Wiese, K. M., & Ridge, K. M. (2015). Influenza A virus infection, innate immunity, and childhood. *JAMA Pediatrics, 169*(10), 956-963.

Das, K., Aramini, J. M., Ma, L.-C., Krug, R. M., & Arnold, E. (2010). Structures of influenza A proteins and insights into antiviral drug targets. *Nature Structural Molecular Biology, 17*(5), 530-538.

Davis, B. K., Wen, H., & Ting, J. P. (2011). The inflammasome NLRs in immunity, inflammation, and associated diseases. *Annual Review of Immunology, 29*, 707-735.

Eisfeld, A. J., Neumann, G., & Kawaoka, Y. (2015). At the centre: Influenza A virus ribonucleoproteins. *Nature Reviews Microbiology, 13*(1), 28-41.

Gao, Q., Chou, Y. Y., Doganay, S., Vafabakhsh, R., Ha, T., & Palese, P. (2012). The influenza A virus PB2, PA, NP, and M segments play a pivotal role during genome packaging. *Journal of Virology, 86*(13), 7043-7051.

Giampieri, M., Balbi, A., Mazzei, M., La Colla, P., Ibba, C., & Loddo, R. (2009). Antiviral activity of indole derivatives. *Antiviral Research, 83*(2), 179-185.

Goraya, M. U., Wang, S., Munir, M., & Chen, J. L. (2015). Induction of innate immunity and its perturbation by influenza viruses. *Protein Cell, 6*(10), 712-721.

Goubau, D., Schlee, M., Deddouche, S., Pruijssers, A. J., Zillinger, T., Goldeck, M., . . . Reis e Sousa, C. (2014). Antiviral immunity via RIG-I-mediated recognition of RNA bearing 5'-diphosphates. *Nature, 514*(7522), 372-375.

Han, Z., Liang, X., Wang, Y., Qing, J., Cao, L., Shang, L., & Yin, Z. (2016). The discovery of indole derivatives as novel hepatitis C virus inhibitors. *European Journal of Medicinal Chemistry, 116*, 147-155.

Iwasaki, A., & Pillai, P. S. (2014). Innate immunity to influenza virus infection. *Nature Reviews Immunology, 14*(5), 315-328.

Jacobs, S. R., & Damania, B. (2012). NLRs, inflammasomes, and viral infection. *Journal of Leukocyte Biology, 92*(3), 469-477.

Jiang, F., Ramanathan, A., Miller, M. T., Tang, G.-Q., Gale, M., Patel, S. S., & Marcotrigiano, J. (2011). Structural basis of RNA recognition and activation by innate immune receptor RIG-I. *Nature, 479*(7373), 423-427.

Killip, M. J., Fodor, E., & Randall, R. E. (2015). Influenza virus activation of the interferon system. *Virus Research*, 209, 11-22.

Lee, J. H., & Lee, J. (2010). Indole as an intercellular signal in microbial communities. *FEMS Microbiology Reviews, 34*(4), 426-444.

Loo, Y. M., Fornek, J., Crochet, N., Bajwa, G., Perwitasari, O., Martinez-Sobrido, L., . . . Gale, M., Jr. (2008). Distinct RIG-I and MDA5 signaling by RNA viruses in innate immunity. *Journal of Virology, 82*(1), 335-345.

Medzhitov, R. (2001). Toll-like receptors and innate immunity. *Nature Review Immunology, 1*(2), 135-145.

Mehta, D. S., Sikotra, K. H., & Shah, V. H. (2005). Synthesis and biological screening of some new novel indole derivatives. *The Indian Journal of Chemistry, 44B*(2594-2597).

Nakagawa, Y., Oda, K., & Nakada, S. (1996). The PB1 subunit alone can catalyze cRNA synthesis, and the PA subunit in addition to the PB1 subunit is required for viral RNA synthesis in replication of the influenza virus genome. *Journal of Virology, 70*(9), 6390-6394.

Olgen, S., Altanlar, N., Karatayli, E., & Bozdayi, M. (2008). Antimicrobial and antiviral screening of novel indole carboxamide and propanamide derivatives. *Zeitschrift fur Naturforschung C, 63*(3-4), 189-195.

Ozdemir, A., Altintop, M. D., Turan-Zitouni, G., Ciftci, G. A., Ertorun, I., Alatas, O., & Kaplancikli, Z. A. (2015). Synthesis and evaluation of new indole-based chalcones as potential antiinflammatory agents. *European Journal of Medicinal Chemistry, 89*, 304-309.

Pham, A. M., Santa Maria, F. G., Lahiri, T., Friedman, E., Marié, I. J., & Levy, D. E. (2016). PKR transduces MDA5-dependent signals for type I IFN induction. *PLOS Pathogens, 12*(3).

Pielak, R. M., Schnell, J. R., & Chou, J. J. (2009). Mechanism of drug inhibition and drug resistance of influenza A M2 channel. *Proceedings of the National Academy of Sciences United States of America, 106*(18), 7379-7384.

Rehwinkel, J., Tan, C. P., Goubau, D., Schulz, O., Pichlmair, A., Bier, K., . . . Reis e Sousa, C. (2010). RIG-I detects viral genomic RNA during negative-strand RNA virus infection. *Cell, 140*(3), 397-408.

Sabbah, A., Chang, T. H., Harnack, R., Frohlich, V., Tominaga, K., Dube, P. H., . . . Bose, S. (2009). Activation of innate immune antiviral responses by Nod2. *Nature Immunology, 10*(10), 1073-1080.

Samji, T. (2009). Influenza A: Understanding the viral life cycle. *The Yale Journal of Biology and Medicine, 82*(4), 153-159.

Segovia, J., Sabbah, A., Mgbemena, V., Tsai, S.-Y., Chang, T.-H., Berton, M. T., . . . Bose, S. (2012). TLR2/MyD88/NF-κB pathway, reactive oxygen species, potassium efflux activates NLRP3/ASC inflammasome during respiratory syncytial virus infection. *PLOS ONE, 7*(1), e29695.

Takeda, K., & Akira, S. (2005). Toll-like receptors in innate immunity. *International Immunology, 17*(1), 1-14.

Thorlund, K., Awad, T., Boivin, G., & Thabane, L. (2011). Systematic review of influenza resistance to the neuraminidase inhibitors. *BMC Infectious Diseases, 11*, 134.

Ting, J. P., Lovering, R. C., Alnemri, E. S., Bertin, J., Boss, J. M., Davis, B. K., . . . Ward, P. A. (2008). The NLR gene family: A standard nomenclature. *Immunity, 28*(3), 285-287.

Tissari, J., Siren, J., Meri, S., Julkunen, I., & Matikainen, S. (2005). IFN-alpha enhances TLR3-mediated antiviral cytokine expression in human endothelial and epithelial cells by up-regulating TLR3 expression. *Journal of Immunology, 174*(7), 4289-4294.

Trinchieri, G. (2010). Type I interferon: Friend or foe? *The Journal of Experimental Medicine, 207*(10), 2053-2063.

Versteeg, G. A., and Garcia-Sastre, A. (2011). *Virus and interferon: Influenza virus and interferons* (pp. 198-199). Norfolk, UK: Caister Academic Press.

Wong, W. Y., Loh, S. W., Ng, W. L., Tan, M. C., Yeo, K. S., Looi, C. Y., . . . Ea, C. K. (2015). A cell-based screening system for anti-influenza A virus agents. *Scientific Reports, 5*, 8672.

Xue, S., Ma, L., Gao, R., Li, Y., & Li, Z. (2014). Synthesis and antiviral activity of some novel indole-2-carboxylate derivatives. *Acta Pharmaceutica Sinica B, 4*(4), 313-321.

Zhang, M.-Z., Chen, Q., & Yang, G.-F. (2015). A review on recent developments of indole-containing antiviral agents. *European Journal of Medicinal Chemistry, 89*, 421-441.

Zhao, F., & Liu, Z. Q. (2009). Indole and its alkyl-substituted derivatives protect erythrocyte and DNA against radical-induced oxidation. *Journal of Biochemical and Molecular Toxicology, 23*(4), 273-279.

LIST OF PUBLICATIONS AND PAPERS PRESENTED

LIST OF PUBLICATIONS:

1. **Tan, M. C.**, Wong, W. Y., Ng, W. L., Yeo, K. S., Mohidin, T. B. M., Lim, Y.-Y., Lafta, F., Ali, H. M., & Ea, C.-K. (2017). Identification of 5-methoxy-2-(Diformylmethylidene)-3,3-dimethylindole as an anti-influenza A virus agent. PLOS ONE, *12*(1), e0170352.

LIST OF PAPER PRESENTED:

1. **Tan, M. C.**, Wong, W. Y., Lafta, F., Ali, H. M., Lim, Y.-Y., & Ea, C.-K., Biological screening for anti-influenza A Virus (IAV) agents, 20th Biological Sciences Graduate Congress (20th BSGC), December, 2015. Thailand.